Research paper

# Analysis of structural damage using simulation and experimental studies in the explosion pit at Kumamoto University

Masatoshi Nishi*†, Masahide Katayama**·***, and Kazuyuki Hokamoto***

*Kumamoto National College of Technology, 2627, Hirayamashinmachi, Yatsushiro City, Kumamoto 866-8501, JAPAN
Phone : +81-965-53-1285
†Corresponding author : nishima@kumamoto-nct.ac.jp

**ITOCHU Techno-Solutions Corporation, 3-2-5, Kasumigaseki, Chiyoda-ku, Tokyo 100-6080, JAPAN

***Kumamoto University, 2-39-1, Kurokami, Chuo-ku, Kumamoto City, Kumamoto 860-8555, JAPAN

Received : November 13, 2014 Accepted : September 3, 2015

406

## Abstract

This study investigates the effect of impulsive pressure on structure damage driven by the detonation of an explosive. A numerical analysis of the explosion pit at the Institute of Pulsed Power Science of Kumamoto University was performed. Though many studies using the explosive PAVEX have been conducted at the pit, a numerical model of this explosion has not been developed. Therefore, the possibility of the use of ANFO data instead of PAVEX was investigated through the numerical analysis AUTODYN-code. The analytical results suggested that damage in the pit was expected at the top and circumferential wall parts. The positions of observed cracks corresponded well with the predictions made in the numerical analysis.

***Keywords*** : explosion pit, structural damage, blast wave, TNT equivalence, numerical simulation.

## 1. Introduction

There are few circumstances in which designing and constructing an explosion pit is possible, and therefore there is limited knowledge regarding how and where explosive damage occurs. It is important to understand these events, especially for the purposes of safety design, and thus the present investigation was conducted using an explosion pit located at the Institute of Pulsed Power Science, Kumamoto University, built in 2001. The structure of this pit is egg-type, formed by hemispheres in the upper and lower parts, welded to a cylindrical center structure. Similar pits have been constructed at AIST (National Institute of Advanced Industrial Science and Technology), Tsukuba, Japan and other institutions due to the good durability and performance of this design. Previous studies on the damage of such explosion pits have been made by Duffey and Romero[1], Pastrnak and co-workers[2] and Nishi and co-workers[3].

The explosion pit at Kumamoto University is built from reinforced concrete, covered with a steel inner wall 25 mm thick. After more than 10 years of service, detonating up to about 1 kg of explosives, some damage appearing in the reinforced concrete has been confirmed[3]. The damage appears as minor cracks, though has the potential to be serious, or lead to serious damage. We conducted a numerical simulation considering the use of TNT explosives in previous research[3].

In the present investigation, the authors choose to investigate the effects of the explosive PAVEX, produced by Kayaku Japan Co., Ltd. mainly composed of ammonium nitrate, which has been used in much of the research undertaken at the explosion pit[4-6]. Additionally, the effects of a similar type of explosive, ANFO, have been investigated.

Due to a lack of available public information regarding PAVEX, the authors have used the available data from ANFO to develop a numerical simulation using the software ANSYS AUTODYN and then confirmed the

validity of the use of the ANFO data through TNT equivalence[7], calculated by the measured static pressure values and simulated results. Then, pressure profiles (total pressure) of the simulated results for ANFO and the measured results for PAVEX explosions in the pit were compared. The results confirmed the validity of using the ANFO data instead of PAVEX for the numerical simulation. Finally, the deformation of the steel wall and the damage observed on the concrete wall in the pit were numerically analyzed.

## 2. Experimental setup

Figure 1 shows a cross-sectional drawing of the explosion pit under consideration ; the experimental setup is also illustrated, including the detonation point at the center of the pit and the position of the pressure sensors. The height of the pit is 9.5 m (buried 3.8 m underground) and the diameter is 7.5 m. The structure is constructed from reinforced concrete covered with a steel plate 25 mm thick. The minimum thickness of the overhead concrete wall and the circumferential walls is 0.5 m.

For the measurement experiments, a PAVEX explosive was placed at the geometric center of the chamber and was ignited using an electric detonator #8. The mass of PAVEX explosive used in the two tests was 0.6 kg and 0.8 kg. Pressure transducers 113B23 made by PCB Piezotronics Inc. were used to measure the blast pressure. The ICP signal conditioner and the oscilloscope were the 480E09 and DPO7054, respectively, both made by Tektronix. The pressure transducers were set at a horizontal distance of 1.5 m to measure static pressure and at 3.25 m on the wall to measure the total pressure.

## 3. Numerical simulation

A two-dimensional axial symmetry model, which simplified the structure, was used for the numerical simulation. Judging from the junction conditions for its shape and the lesser effect on exterior cracks, this analytical model disregards pit internal structures, such as H-shaped steel girders and grating.

In this model, the pit's steel interior was simulated by the Shell elements. The material of steel was 4340 steel and the Johnson-Cook constitutive law[8] was applied written as the following, where the parameters are listed

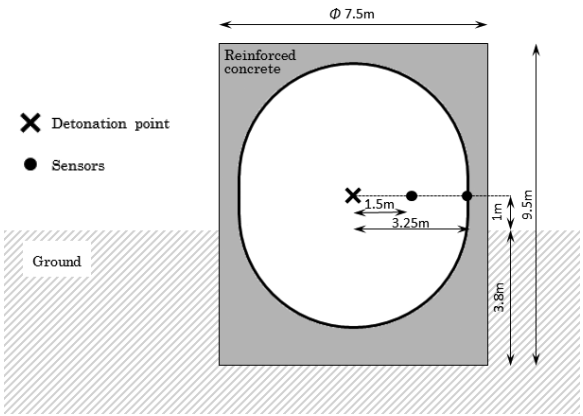


**Figure 1** Setup of experiments in the explosion pit.

**Table 1** Johnson-Cook parameters for 4340 steel.

| Density $\rho$ [kg m$^{-3}$] | Shear modulus $G_0$ [GPa] | $A$ [GPa] | $B$ [GPa] | $N$ | $C$ | $m$ |
|---|---|---|---|---|---|---|
| $2.785 \cdot 10^3$ | 81.8 | 0.792 | 0.51 | 0.26 | 0.014 | 1 |

**Table 2** JWL parameters for TNT and ANFO.

| Parameters | $A$ [GPa] | $B$ [GPa] | $R_1$ | $R_2$ | $\omega$ |
|---|---|---|---|---|---|
| TNT explosive | 371 | 3.23 | 4.15 | 0.950 | 0.30 |
| ANFO explosive | 49.5 | 1.89 | 3.91 | 1.12 | 0.33 |

in Table 1.

$$Y = (A + B\varepsilon^n)(1 + C \ln \dot{\varepsilon})(1 - T^m) \quad (1)$$

For simplicity, the concrete was considered as Euler elements. The porous equation of state was used for concrete, as was the Drucker-Prager strength model. The equation of state for the JWL equation[9] for the TNT and ANFO explosives was applied to the model as

$$P = A\left(1 - \frac{\omega\eta}{R_1}\right)\exp\left(-\frac{R_1}{\eta}\right) + B\left(1 - \frac{\omega\eta}{R_2}\right)\exp\left(-\frac{R_2}{\eta}\right) + \omega\eta\rho_0 e \quad (2)$$

with pressure $P$, density $\rho$, specific internal energy $e$, $\eta = \rho/\rho_0$ (where $\rho_0$ is the initial density) and JWL parameters as shown in Table 2. In the simulation, the form of the explosive was column.

Air was assumed as an ideal gas. The ratio of specific heat $\gamma$ ($= c_p/c_v$;$c_p$ : molar specific heat at constant pressure, $c_v$ : molar specific heat at constant volume) is the property value and is expressed by the following equation.

$$p = (\gamma - 1)\rho e \quad (3)$$

where $\gamma = 1.4$, $\rho = 1.225$ kg m$^{-3}$, $e = 2.067 \cdot 105$ J kg$^{-1}$.

## 4. Results and discussion

### 4.1 The validity of the use of ANFO data

The numerical simulation was performed for the TNT and ANFO explosives based on the consideration on the TNT equivalence[7]. As to clarify the validity of our simulated results for TNT, the change in peak overpressure of the explosion with scaled distance was compared with the data by Kingery and Pannill[10] as shown in Figure 2. Note that the blast wave data of Kingery and Pannill[10] was ground surface data, whereas the present numerical simulation approximates the ones in free air. Therefore, the mass of TNT explosive in the numerical simulation was doubled to meet the same requirements as Kingery and Pannill[10], as reported by Nakayama and co-workers[11]. Here, the numerical simulation of the single and double mass of TNT is noted as the numerical simulation of TNT (W) and numerical simulation of TNT (2W), respectively.

In Figure 2, the almost straight solid line indicates the data of Kingery and Pannill[10] and the dotted line is the data obtained by the numerical simulation of TNT (2W).

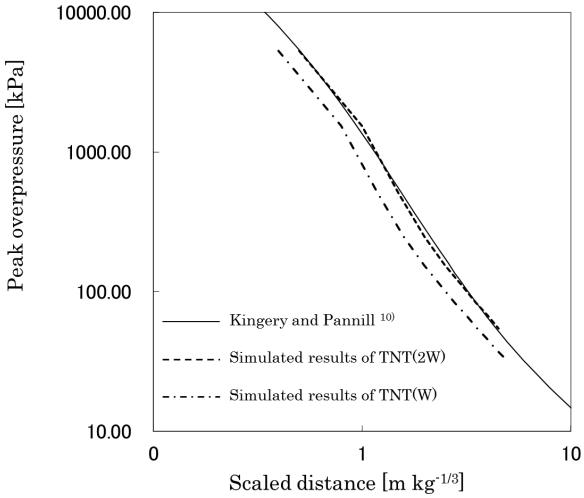


**Figure 2** Blast wave data by Kingery and Pannill[10], compared with simulated results.

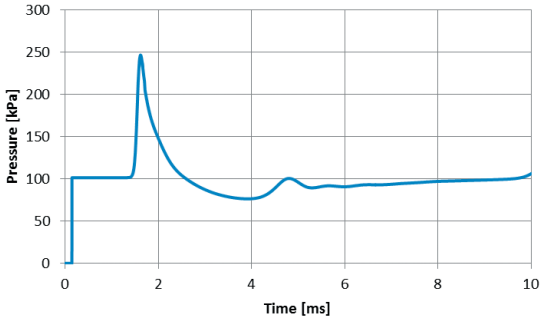


**Figure 3** Simulated static pressure at 1.5 m (0.6 kg ANFO).

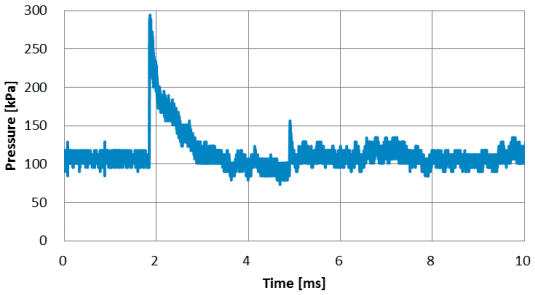


**Figure 4** Experimentally measured static pressure at 1.5 m (0.6 kg PAVEX).

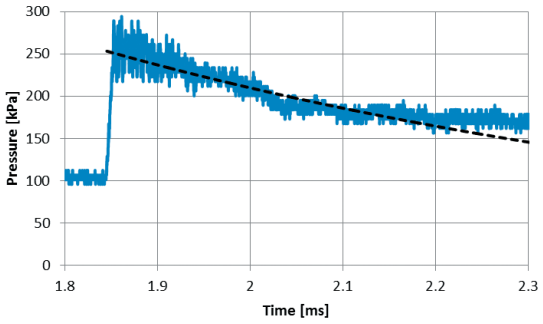


**Figure 5** Enlarged pressure profile of Figure 4 close to peak pressure. Peak pressure was determined by the intersection point of the rise pressure with a smooth correction curve, and with exponential function suggested as dotted line.

**Table 3** The values of simulated results of TNT (W).

| Scaled distance [m kg$^{-1/3}$] | 1.59 | 1.98 | 2.38 | 2.78 | 3.17 | 3.57 | 3.97 | 4.37 | 4.76 |
|---|---|---|---|---|---|---|---|---|---|
| Peak overpressure [kPa] | 246.3 | 154.1 | 110.5 | 83.4 | 67.0 | 54.3 | 45.9 | 39.0 | 34.1 |

The figure shows quite good agreement for the data. Therefore, the numerical simulations were concluded to be reliable. The simulated values of scaled distance and peak overpressure for TNT (W) are cited in Table 3.

Next, the validity of using the ANFO data instead of PAVEX was established by using TNT equivalence based on the simulated results of TNT (W). Static pressure profiles obtained by the simulated and experimental results are shown in Figures 3, 4 and 5.

Figure 3 shows the static pressure obtained through numerical simulation for the case of 0.6 kg of ANFO at 1.5 m from the detonation point. Figure 4 shows the similar data obtained from the same position, instead using 0.6 kg of PAVEX. Figure 5 shows the same graph with an enlarged time scale. The correction value of the peak static pressure, determined by exponential function in Figure 5, is suggested by an arrow in Figure 4, and the peak pressure is quite similar, as found in Figures 3 and 4.

According to these results, the TNT equivalence[7] in terms of peak static pressure and scaled impulse of positive phase was calculated and shown in Table 4. To calculate the TNT equivalence, the values of simulated results of TNT (W) were used. For example, in the case of the mass of PAVEX $W = 0.6$ kg at horizontal distance $a = 1.5$ m from the detonation point, the value of scaled distance $Rs_{TNT}$ was calculated to 2.05 m kg$^{-1/3}$ from Table 3 with interpolation method since static overpressure was 148.6 kPa from Figures 4 and 5. Then, the equivalent mass $W_{eq}$ of TNT explosive for 0.6 kg PAVEX and TNT equivalence $R$ are given in Equations 4 and 5, respectively. The TNT equivalence in terms of impulse can be calculated via a similar process.

$$W_{eq} = \left(\frac{a}{Rs_{TNT}}\right)^3 = 0.392\text{kg} \quad (4)$$

$$R = \frac{W_{eq}}{W} = 0.653 \quad (5)$$

As found in Table 4, it is clear that the results for the PAVEX and ANFO explosives show they are closely in agreement. The values of TNT equivalence were smaller than usual[12] due to the small amount of explosive charge used. Almost same TNT equivalence for the ANFO explosive was reported by Arai and Hiyoshi[13].

Change in the total pressure over time simulated for 0.6 kg of ANFO and measured for 0.6 kg of PAVEX at the steel wall (3.25 m from the center) is shown in Figures 6 and 7, respectively. The measured pressure profile in Figure 7 suggests the second peak pressure comes from the reflection of the blast wave.

Total pressure refers to the sum of static pressure and dynamic pressure $P_{imp}$. In the case of 0.6 kg PAVEX at 3.25 m, the value of scaled distance $Rs_{TNT}$ was obtained as

**Table 4** TNT equivalence for the PAVEX and ANFO explosives based on blast wave parameters at 1.5 m.

| Mass of charge [kg] | PAVEX explosive | | ANFO explosive | |
|---|---|---|---|---|
| | Peak static overpressure | Scaled impulse of positive phase | Peak static overpressure | Scaled impulse of positive phase |
| 0.6 | 0.653 | 0.536 | 0.643 | 0.528 |
| 0.8 | 0.635 | 0.520 | 0.688 | 0.504 |

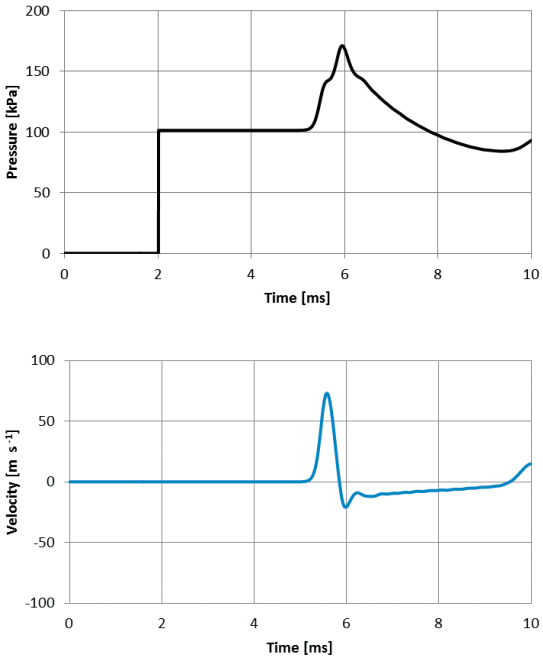


**Figure 6** Simulated total pressure and velocity $u_{imp}$ near steel wall.

follows :

$$Rs_{TNT} = \frac{3.25}{(0.6R)^{1/3}} = 4.44 \text{ m kg}^{-1/3} \quad (6)$$

with TNT equivalence $R$ (Equation 5). The static overpressure was calculated to be 35.6 kPa from Table 3 with interpolation method, and the dynamic overpressure was calculated as follows :

$$P_{imp} = \rho c u_{imp} = 31.1 \text{ kPa} \quad (7)$$

with the speed of sound $c = 340$ m s$^{-1}$ and velocity $u_{imp} \fallingdotseq 75$ m s$^{-1}$ (from simulated results as shown in Figure 6). Therefore, the theoretical value of the total overpressure was 66.7 kPa and this value seems to be the same for Figures 6 and 7. Thus, the total pressure generated by the blast waves of ANFO and PAVEX at the steel wall created nearly identical profiles. Note that the rise time of the pressure obtained through numerical simulation (Figure 6) seems longer due to the limitation of mesh size[14]. As the entire region of computation was much larger than the size of the explosive, a remapping technique[15] was applied because it was difficult to use a consistently small mesh size over the entire region. This technique applied a smaller mesh size at the local region near the detonation point and a larger mesh size over the remainder of the region for improved efficiency in the analysis of blast wave propagation.

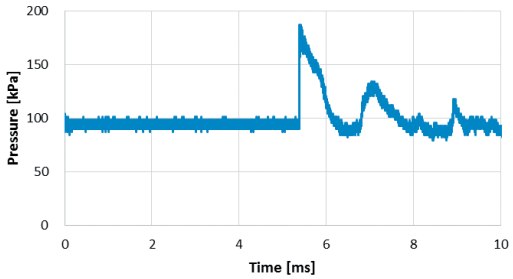


**Figure 7** Measured total pressure at steel wall (3.25 m from center).

According to the above result, comparing the ANFO and PAVEX explosives in terms of TNT equivalence and total pressure profiles, the validity of using ANFO data for the numerical simulation instead of the unavailable PAVEX data was confirmed in this subsection.

### 4.2 The damage of the explosion pit based on numerical simulation

Figure 8 shows the propagation of a blast wave using 1 kg of the ANFO explosive at 2.7 ms, 3.6 ms, 5.1 ms, 8.7 ms, 10 ms and 14.5 ms after ignition. The damage of the concrete at 5.1 ms, 8.7 ms and 20 ms is displayed in Figure 9. Although in the simulation the steel wall, modeled as Shell elements, must join with the concrete part, modeled as Lagrange elements, it is difficult to join the elements due to the shape of the steel wall. In this analysis, concrete was modeled as Euler elements and the reinforcing steel in the concrete was disregarded. The damage points of the concrete were less affected by ignoring the reinforcing steel, and therefore, the damage of the pit as shown in Figure 9 can be regarded as an accurate result[16].

It can be seen that the propagation of the blast wave is spread concentrically as found in Figures 8(a) and 8(b). The small arrows in Figures 8 and 9 suggest the velocity vector of the steel inner wall. The velocity vector is generated outward towards the circumferential direction at the center height of the inner wall at 5.1 ms and there is no damage to the concrete (Figure 8(c) and 9(a)). When the detonation pressure reaches the top and bottom of the chamber at 8.7 ms(Figure 8(d)), the velocity vector at the wall reverses direction, damaging the concrete wall, shown by the red points in Figure 9(b). Such vibrations at the wall and the top and bottom parts are repeated, as shown in Figure 8(e) and 8(f), and the concrete is damaged (Figure 9(c)). The damage of the concrete at the bottom parts was reduced compared to other sections of the pit as the concrete at the bottom is much thicker. The simulated results are substantially the same as the location of damage observed in the pit at the wall and the upper part, as reported earlier[3].

## 5. Conclusion

This study considered the damage to the explosion pit based at Kumamoto University by developing a numerical

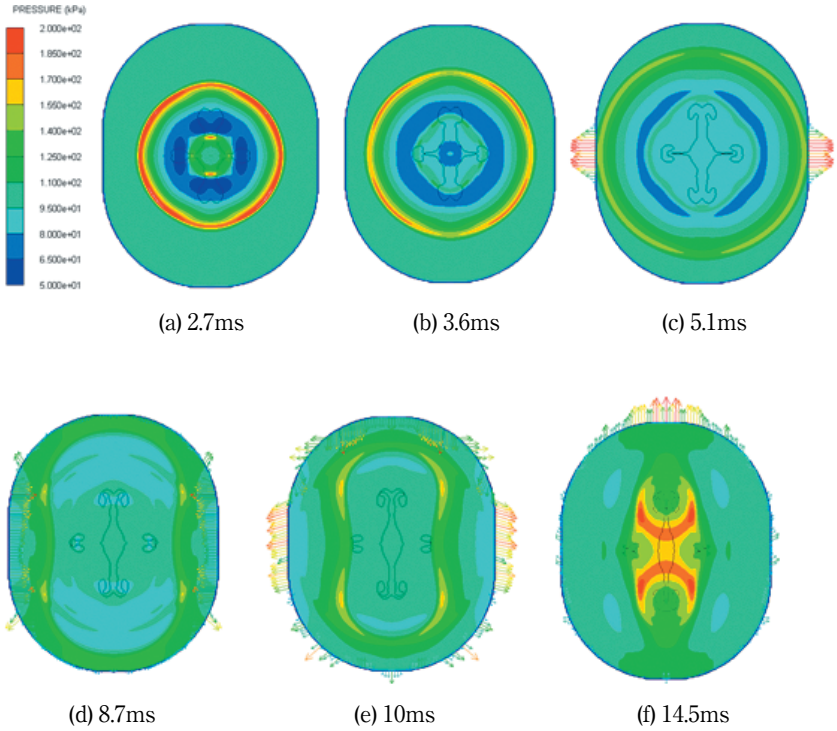


(a) 2.7ms (b) 3.6ms (c) 5.1ms

(d) 8.7ms (e) 10ms (f) 14.5ms

**Figure 8** Propagation of blast wave based on numerical simulation (1 kg ANFO). Concrete part is not displayed.

simulation for the PAVEX explosive, which is commonly used in studies at the pit. After confirming the validity of using data from the similar explosive ANFO instead of unavailable PAVEX data, the damage caused in the explosion pit for 1 kg of ANFO was investigated, showing the weakness at top and wall parts where the concrete areas are thinner.

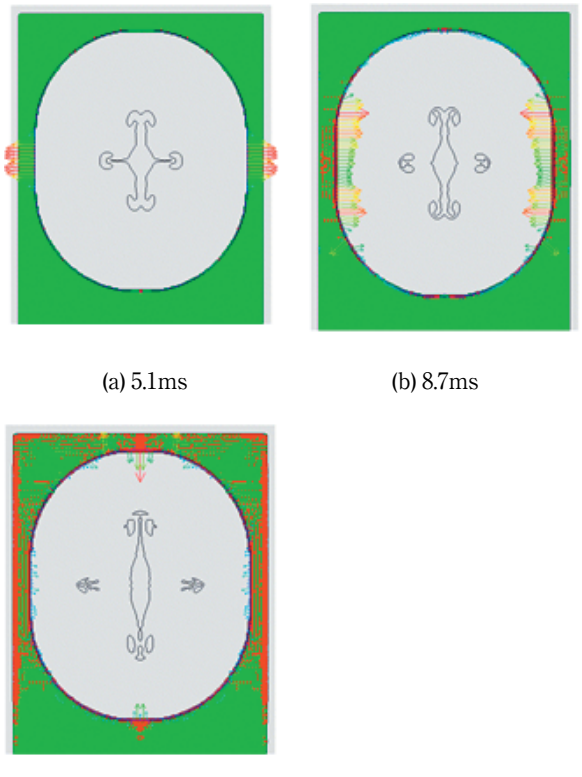

(a) 5.1ms (b) 8.7ms

(c) 20ms

**Figure 9** Damage of explosion pit based on numerical simulation (1 kg ANFO).

## Acknowledgement

The authors are grateful to the financial support provided by The foundation for the Promotion of the Industrial Explosives Technolongy (2013).

## References

1) T. A. Duffey and C. Romero, Int. J. Impact Eng., 28, 967 – 983 (2003).
2) J. W. Pastrnak, C. D. Henning, V. A. Switzer, W. Grundler, J. R. Holloway, J. J. Morrison, and R. S. Hafner, Report UCRL-CONF – 205421, American Society of Mechanical Engineers (2004).
3) M. Nishi, M. Katayama, and K. Hokamoto, Mater. Sci. Forum, 767, 150 – 153 (2013).
4) Y. Morizono, T. Fukuyama, M. Matsuda, and S. Tsurekawa, Mater. Trans., 52, 2178 – 2183 (2011).
5) K. Hokamoto, M. Vesenjak, and Z. Ren, Mater. Lett., 137, 323 – 327 (2014).
6) P. Manikandan, K. Hokamoto A. A. Deribas, K. Raghukandan, and R. Tomoshige, Mater. Trans., 47, 2049 – 2055 (2006).
7) Y. Nakayama, M. Yoshida, Y. Kakudake, M. Iida, N. Ishikawa, K. Kato, H. Sakai, S. Usuda, K. Aoki, N. Kuwabara, K. Tanaka, K. Tanaka, and S. Fujiwara, Kogyo Kayaku (Sci. Tech. Energetic Materials), 50, 88 – 92 (1989) (in Japanese).
8) M.A Meyers, "Dynamic Behavior of Materials", Wiley Inter science (1994).
9) B.M. Dobratz, "LLNL Handbook of Explosives", UCRL – 52997, Lawrence Livermore National Laboratory (1981).
10) C. N. Kingery and B. F Pannill, BRL Memorandum Report No.1518 (1964).
11) M. Yoshida and Y. Nakayama, EXPLOSION, 17, 2 – 5 (2007) (in Japanese).

12) J. L. Maienschein, "Estimating Equivalency of Explosives Through A Thermochemical Approach", U.S. Department of Energy (2002).
13) H. Arai and R. Hiyoshi, Sci. Tech. Energetic Materials, 71, 1 − 8 (2011) (in Japanese).
14) M. Katayama and K. Tanaka, Symposium on Shock Waves in Japan, 257 − 260 (2003) (in Japanese).
15) M. Katayama, M. Itoh, S. Tamura, M. Beppu, and T. Ohno, Int. J. Impact Eng., 34, 1546 − 1561 (2007).
16) Japan Nuclear Energy Safety Organization, "ATOM Library (NRA Library)", https : //www.nsr.go.jp/archive/jnes/atom-library/H13_9_8.pdf, (accessed : 5 − May − 2015) (online) (in Japanese).